

pubs.acs.org/ac Article

# Effects of Cascading Optical Processes: Part III. Impacts on Spectroscopic Measurements of Fluorescent Samples

Max Wamsley, Pathum Wathudura, Samadhi Nawalage, Shengli Zou, and Dongmao Zhang



Cite This: Anal. Chem. 2023, 95, 10279-10288



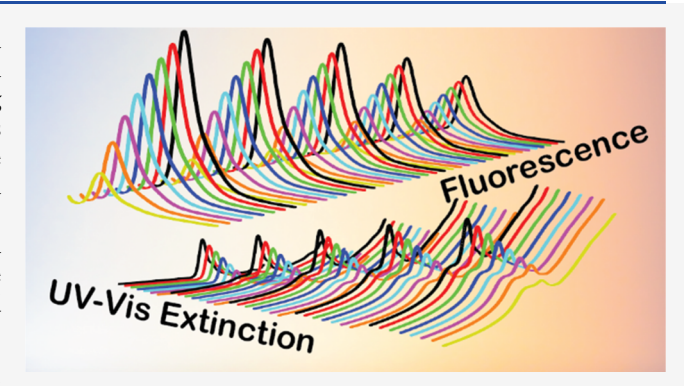
**ACCESS** I

Metrics & More

Article Recommendations

Supporting Information

ABSTRACT: Cascading optical processes involve sequential photon—matter interactions triggered by the same individual excitation photons. Parts I and II of this series explored cascading optical processes in scattering-only solutions (Part I) and solutions with light scatterers and absorbers but no emitters (Part II). The current work (Part III) focuses on the effects of cascading optical processes on spectroscopic measurements of fluorescent samples. Four types of samples were examined: (1) eosin Y (EOY), an absorber and emitter; (2) EOY mixed with plain polystyrene nanoparticles (PSNPs), which are pure scatterers; (3) EOY mixed with dyed PSNPs, which scatter and absorb light but do not emit; and (4) fluorescent PSNPs that are simultaneous light absorbers, scatterers, and emitters. Interference from both forward scattered



and emitted photons can cause nonlinearity and spectral distortion in UV—vis extinction measurements. Sample absorption by nonfluorogenic chromophores reduces fluorescence intensity, while the effect of scattering on fluorophore fluorescence is complicated by several competing factors. A revised first-principles model is developed for correlating the experimental fluorescence intensity with the sample absorbance in solutions containing both scatterers and absorbers. The optical properties of fluorescent PSNPs of three different sizes were systematically investigated by using integrating-sphere-assisted resonance synchronous spectroscopy, linearly polarized resonance synchronous spectroscopy, UV—vis, and fluorescence spectroscopy. The insights and methodology provided in this work should help improve the reliability of spectroscopic analyses of fluorescent samples, where the interplay among light absorption, scattering, and emission can be complex.

## ■ INTRODUCTION

Cascading optical processes refer to two or more sequential optical events triggered by individual excitation photons. Such sequential optical events can be of the same (e.g., scattering of the scattered photons) or different mechanistic origins (e.g., emission after absorption). Parts I and II of these three companion articles presented the cascading optical processes in scattering-only samples (Part I) and solutions that contain both scatterers and absorbers but not emitters (Part II).<sup>1,2</sup> While the cascading optical process in scattering-only samples is relatively simple, as it involves only multiple scatterings, its impact on spectroscopic measurements is significant. It complicates scattering extinction, intensity, and depolarization analysis even when the sample concentration is within the linear dynamic range (LDR) of the UV—vis spectrophotometer.<sup>1,3,4</sup>

The interplay between light absorption and scattering adds complexity to cascading optical processes in samples that contain both light absorbers and scatterers, making it far more complicated compared to scatterer-only solutions.<sup>2</sup> Light absorption invariably reduces the scattering intensity due to the absorption inner-filter effect (IFE).<sup>5-7</sup> However, the impact of scattering on light absorption is complicated

depending on whether the scattered light is taken into consideration. Scattering reduces light absorption along the linear optical path from the excitation source to the UV—vis detector. However, absorption of the scattered photons can partially, totally, and even overcompensate for such reduced light absorption. Imaginably, the degree to which the scattered light is absorbed depends not only on the solution volume, sample absorption, and scattering activities but also the cuvette geometry. In Part II, we systematically examined the impact of scattering on the total light absorption, including the absorption of the scattered photons for samples with a solution volume of 3 mL in a 1 cm square cuvette. In such a case, the total light absorption of the scatterer-containing samples is approximately the same as their respective scatterer-free counterparts, with the same absorption extinction.<sup>2</sup> The

Received: February 23, 2023 Accepted: June 12, 2023 Published: June 29, 2023





presence of scatterers in those samples changes the locations where light absorption occurs but does not significantly modify the amount of light absorbed.<sup>2</sup>

The present work (Part III) focuses on the cascading optical processes in fluorescent solutions and their impacts on sample UV-vis, scattering, and fluorescence measurements. Mechanistically, the cascading optical processes in fluorescent samples can be extraordinarily complicated. Even for solutions containing only one molecular fluorophore, there are two sequential optical events: absorption and emission. Numerous additional cascading processes can occur if the fluorophore also absorbs at the emission wavelengths. In this case, the emitted photons can be reabsorbed, possibly triggering further emission, reabsorption, and so on. In scatterer-containing fluorescent samples, the complexity of the cascading optical processes grows exponentially because scattering can perturb the optical path of excitation and emission photons inside the solutions, consequently affecting the fluorescence signal generation and/or detection.

$$I^{corr}(\lambda_x, \lambda_m) = I(\lambda_x, \lambda_m) \times 10^{0.5A_x + 0.5A_m}$$
(1)

$$I^{corr}(\lambda_x, \lambda_m) = I(\lambda_x, \lambda_m) \times 10^{d_x A_x + d_m A_m}$$
 (2)

Existing work on the effects of cascading optical processes on fluorescence measurements has almost exclusively been on the impacts of fluorophore or sample absorption on the fluorescence intensity. Absorption causes nonlinearity between fluorescence intensity and fluorophore concentration, as well as introduces spectral distortion.<sup>7-9</sup> Such effects have been commonly referred to as the absorption IFE. 5,9-11 Many mathematical models have been developed for correcting the absorption IFE on fluorescence measurements. Equation 1 has been popularly used for correcting the absorption IFE on fluorescence spectra acquired with a 1 cm square cuvette.  $A_x$ and  $A_m$  are the sample absorbances, quantified using a 1 cm path length cuvette, at the excitation and emission wavelengths, respectively.<sup>5</sup> This model (eq 1) assumes that the instrument is perfectly aligned, so that the effective excitation and emission path lengths are both 0.5 cm in the conventional 90° spectrofluorometric spectral acquisition.

We previously reported a generalized model for correcting the absorption IFE on fluorescence measurements (eq 2), where  $d_x$  and  $d_m$  refer to the effective light absorption and emission path lengths. These path lengths can be readily quantified using a solvent Raman technique. This model is also useful for correcting the absorption IFE on resonance synchronous spectra acquired with a spectrofluorometer. Since the excitation and detection wavelengths are the same in these spectroscopic measurements, the total absorption path length is simply the sum of  $d_x$  and  $d_m$ .

The effectiveness of eq 2 for correcting the absorption IFE has been extensively demonstrated with molecular fluorophores containing no significant scattering. The absorption IFE-corrected fluorescence intensity exhibits excellent linearity with fluorophore concentration. However, current knowledge of the effects of light scattering on fluorescence intensity has been scant. We have previously compared the effects of sample absorption and scattering on fluorophore fluorescence and concluded that, in comparison to absorption, the impact of scattering on sample fluorescence intensity is negligibly small. However, this conclusion was derived with polystyrene nanoparticles (PSNPs) of 100 nm in diameter. The overall generality of this observation is unknown. Addressing this

question is important since the impacts of multiple scattering on spectroscopic measurements depend strongly on particle sizes.

Four types of samples are used in this study, including (1) eosin Y (EOY), a molecular fluorophore with no significant scattering activity; (2) EOY mixed with plain polystyrene nanoparticles (PSNPs) that are pure scatterers; (3) EOY mixed with dyed PSNPs that are scattering and absorbing, but not emitting nanoparticles; and (4) fluorescent PSNPs that are composed of fluorescent dyes impregnated inside PSNPs. The first group of samples is simultaneous light absorbers and emitters with no significant scattering activities, while the remaining three are simultaneous light absorbers, scatterers, and emitters.

The present work focuses on the following three specific objectives. First, we demonstrate the potential pitfalls in UVvis measurements of fluorescent samples. Parts I and II showed how the interference of forward scattered light can cause the experimental UV-vis extinction to deviate from Beer's law even when the sample theoretical extinction is within the LDR of the used UV-vis instrument. Imaginably, forward propagated fluorescence can also cause similar interference. Second, by using a series of PSNPs with varied sizes and optical properties, we wish to establish a systematic understanding of the effects of light scattering on fluorophore fluorescence intensity and depolarization. Third, we wish to provide a general guideline for experimental investigation on the optical properties of fluorescence nanoparticles that have become increasingly popular in chemical, biological, and materials research. There are numerous problematic interpretations of the spectra acquired with these samples, including assigning sample UV-vis extinction spectra as absorbance without considering scattering contribution and ineffective correction of absorption IFE on the fluorescence and scattering measurements. 19-23 Addressing these issues is important for a wide range of scientific inquiries, given the importance of fluorescence in education, research, and technological developments.

## **■ EXPERIMENTAL SECTION**

Materials and Equipment. Polybead carboxylate polystyrene nanoparticles (PSNPs), red dyed polystyrene nanoparticles (dPSNPs), and fluorescent polystyrene nanoparticles (fPSNPs) were purchased from Polysciences, Inc. PSNPs with diameters of 100 nm (catalog #16688-15), 200 nm (catalog #08216-15), and 380 nm (catalog #21753-15) were abbreviated as PSNP<sub>100</sub>, PSNP<sub>200</sub>, and PSNP<sub>380</sub>, respectively. The dPSNP with a diameter of 530 nm (catalog #19815-15) was abbreviated as dPSNP<sub>530</sub>. fPSNPs with diameters of 43 nm (catalog #16661-10), 95 nm (catalog #17150-10), and 180 nm (catalog #09834-10) were abbreviated as fPSNP<sub>43</sub>, fPSNP<sub>95</sub>, and fPSNP<sub>180</sub>, respectively. Bright field and fluorescence photographs of PSNP, dPSNP, and fPSNP solutions are shown in the Supporting Information (Figure S1). Analytical grade eosin Y (EOY) and potassium permanganate (KMnO<sub>4</sub>) were obtained from Sigma-Aldrich and used as received without further purification. Nano pure water (18.2 M $\Omega$  cm<sup>-1</sup>, Thermo Scientific) was used for all sample preparations. For simplicity, the EOY and PSNP nanoparticle mixture was abbreviated as EOY/PSNP.

A Shimadzu UV-2600i spectrophotometer with an ISR 2600 integrating-sphere accessory (Duisburg, Germany) was used for all UV-vis and integrating-sphere UV-vis (ISUV) spectra.

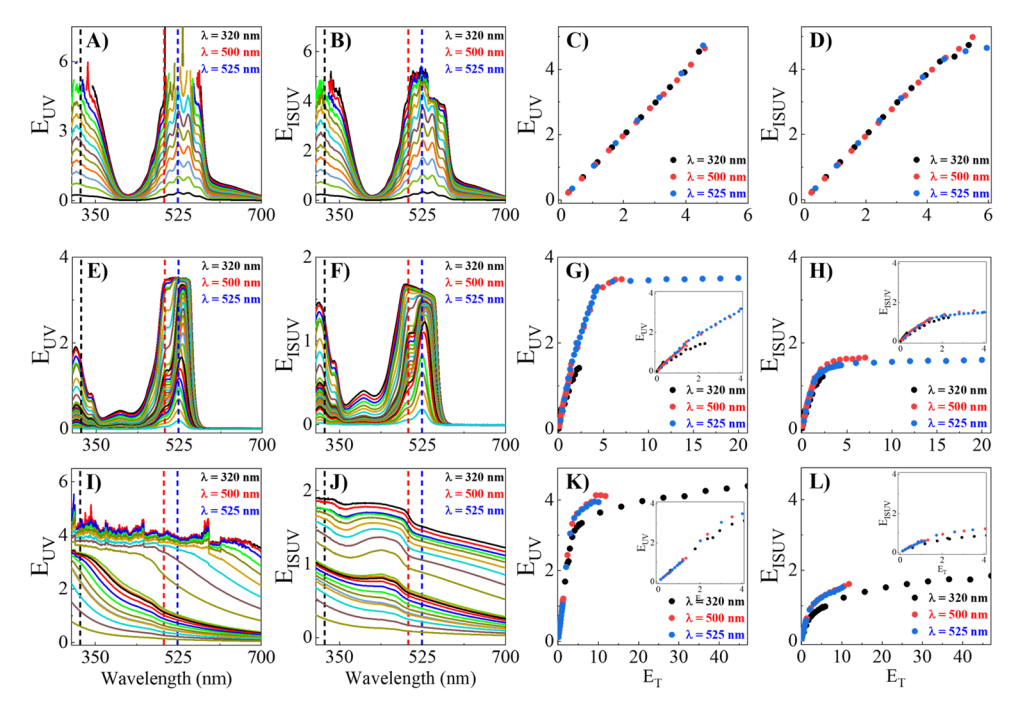


Figure 1. (A, E, I) UV-vis spectra, (B, F, J) ISUV spectra, (C, G, K) UV-vis extinction as a function of the sample theoretical extinction, and (D, L) ISUV extinction as a function of the sample theoretical extinction for (A-D) KMnO<sub>4</sub> from 0.14 to 3.62 mM, (E-H) EOY from 1.67 to 169.08  $\mu$ M in ethanol, and (I-L) fPSNP<sub>180</sub> from 0.01 to 1.01 nM. The evaluated wavelengths and the trend lines are color coded. Only the data obtained with a theoretical extinction lower than 4.3 are shown in the trend lines.

Fluorescence spectra and the resonance synchronous spectra were obtained using a Fluoromax-4 spectrophotometer (Horiba Jobin Yvon, Edison, NJ, U.S.A.). A K-Sphere Petite integrating-sphere (Horiba PTI) with an internal diameter of 80 mm and a neutral density filter with an optical density of 2.0  $\pm$  0.05 from 200 to 1100 nm (Thorlabs) was used for all integrating-sphere-assisted resonance synchronous spectroscopy (ISARS) spectral acquisition.

**Spectroscopic Measurements.** All spectrofluorometer-based spectra were acquired with an integration time of 0.3 s and a bandwidth of 2 nm for both excitation and emission monochromators. The G factor spectrum for correcting the polarization bias was quantified in a previous study. All of the spectra for the measurements were obtained using a 1 cm Thorlabs UV-fused quartz cuvette with a sample volume of 3 mL at room temperature. A neutral density filter with an optical density of  $2.0 \pm 0.05$  from 200 to 1100 nm (Thorlabs) was used for the fluorescence spectral acquisition of all of the EOY samples unless specified.

### RESULTS AND DISCUSSION

**UV–Vis Extinction.** Parts I and II showed that forward scattered light can interfere with the UV–vis extinction spectra of scatterer-containing samples. In Such an interference can cause the measured UV–vis intensity to deviate from Beer's law even when the sample theoretical extinctions are within the instrument LDR that is quantified by using molecular chromophores. Imaginably, forward fluorescence photons can also reach the UV–vis detector, introducing spectral interference. A generalized model for illustrating how scattering and fluorescence interference can interfere with the UV–vis extinction measurement is developed for analytes that are assumed to be simultaneous scatterers, absorbers, and emitters at the excitation wavelength. In this case, the sample experimental UV–vis extinction intensity  $E_{UV}(\lambda_x)$  can be

parametrized using eq 3. A detailed mathematical derivation is shown in the Supporting Information.

$$E_{UV}(\lambda_x) = -\log \left[ \left( I_o(\lambda_x) 10^{-E_T(\lambda_x)} + \eta_s I_{S,fw}(\lambda_x) + \eta_F \int_0^\infty I_{F,fw}(\lambda_x, \lambda_m) d\lambda_m \right) / \left( I_O(\lambda_x) \right) \right]$$
(3)

 $E_T(\lambda_x)$  is the theoretical extinction of the sample, which is the sum of the sample theoretical absorption and scattering extinction.  $I_0(\lambda)$  is the excitation intensity. The integration in the fluorescence term is necessary, as the fluorescence emission usually spans a broad wavelength range. Since the conventional UV—vis spectrophotometer uses only excitation wavelengths, with no detection monochromator, fluorescence emission at any wavelength can interfere with UV—vis measurements.  $\eta_S$  and  $\eta_F$  refer to the fraction of the forward scattered light  $I_{S,fw}(\lambda_x)$  and emitted light  $\int_0^\infty I_{F,fw}(\lambda_x, \lambda_m) \ d\lambda_m$ , respectively, reaching the UV—vis detector. These values depend on the collection angle of the UV—vis detector and the spatial distribution of the scattered and emitted photons.  $I_{S,fw}(\lambda_x)$ 

Equation 3 can be simplified for predicting the scattering or fluorescence interference with sample UV—vis measurements, including the equations presented in Part I for samples that contain only light scatterers, and in Part II where analytes are simultaneous absorbers and scatterers. For the simplest fluorescent samples that contain only molecular fluorophores with no significant scattering activities, eq 3 is simplified into eq 4.

$$E_{UV}(\lambda_x) = -\log \frac{I_o(\lambda_x) 10^{-A_T(\lambda_x)} + \eta_F \int_0^\infty I_{F,fw}(\lambda_x, \lambda_m) d\lambda_m}{I_O(\lambda_x)}$$
(4)

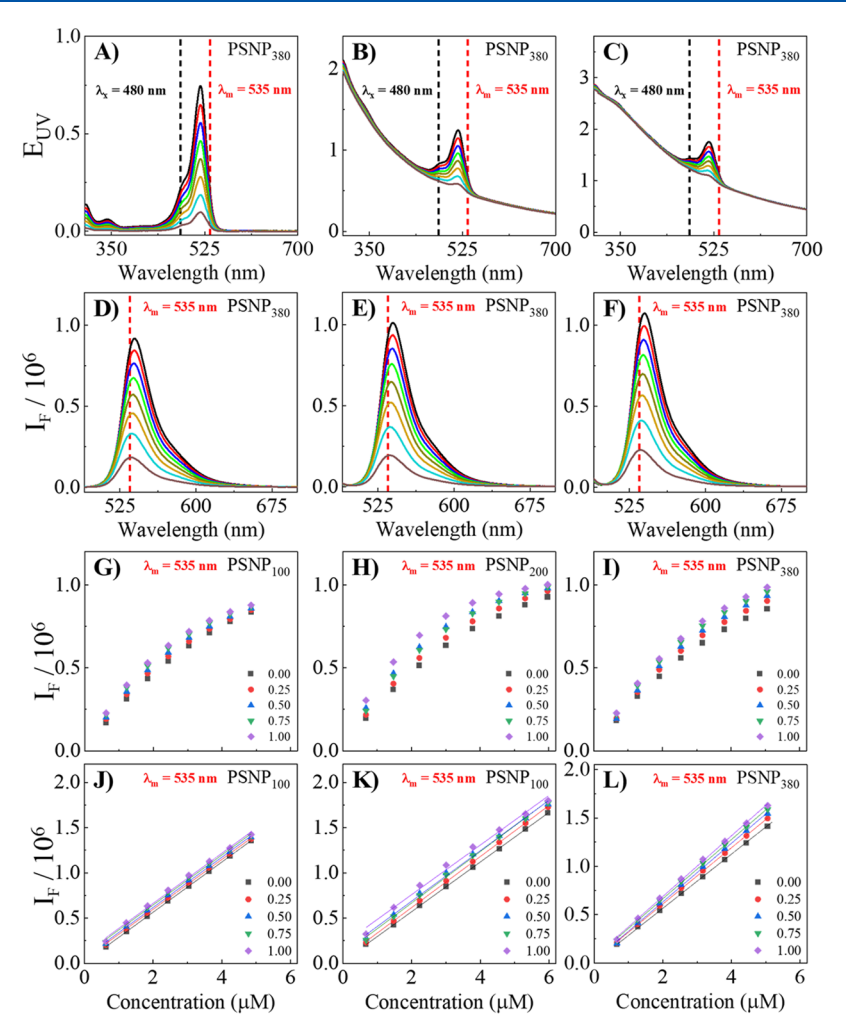


Figure 2. (A–C) UV–vis and (D–F) fluorescence spectra of (A, D) EOY and (B, E), (C, F) EOY/PSNP<sub>380</sub> solutions. The PSNP<sub>380</sub> concentrations for the samples shown in (A, D), (B, E), and (C, F) are 0, 3.83, and 7.69 pM, respectively. The EOY concentrations in each series are the same (0.68, 1.48, 2.23, 3.0, 3.8, 4.6, 5.3, to 6.0 μM). The excitation wavelength is 480 nm for the fluorescence spectra shown. (G–I) Asacquired fluorescence intensity at 535 nm as a function of EOY concentration for EOY/PNSP<sub>100</sub>, EOY/PNSP<sub>200</sub>, and EOY/PSNP<sub>380</sub>, respectively. The legend shows the nominal PSNP scattering extinction in EOY/PSNP solutions. (J–L) Absorption IFE-corrected fluorescence intensity as a function of EOY concentration for the data shown in (G–I). The solid lines shown are obtained by linear curve fitting. Complete data obtained with EOY/PSNP<sub>100</sub>, EOY/PSNP<sub>200</sub>, and EOY/PSNP<sub>380</sub> are shown in Figures S4–S6.

We demonstrated earlier that the forward scattered light causes a deviation of experimental UV-vis intensity from Beer's law.<sup>1,2</sup> However, eq 3 and eq 4 show that the forward scattered and fluorescence light also introduces spectral distortion due to the fact that the degree of scattering and fluorescence interference can be strongly wavelength dependent. Such interferences are shown with the extinction spectra acquired with both the conventional UV-vis and the recently reported ISUV method for KMnO<sub>4</sub>, EOY, and dPSNP<sub>180</sub> (Figure 1). The experimental UV-vis spectra of KMnO<sub>4</sub> solutions and their corresponding ISUV spectra are the same (Figure 1A–D). The experimental extinctions are the same as their theoretical extinction intensities for the evaluated wavelengths for the samples with theoretical extinctions below 4, which is considered the upper LDR limit of the used spectrophotometer. This datum is not surprising because KMnO<sub>4</sub> is approximately a pure light absorber with no significant light scattering. However, the conventional UV-vis spectra and their corresponding ISUV spectra are remarkably different from both EOY (Figure 1E-H) and fPSNP<sub>180</sub> (Figure 1I-L). Nonlinearity appears in the conventional

UV—vis measurements even when the theoretical EOY and fPSNP samples are significantly lower than 4. Since EOY differs from KMnO<sub>4</sub> only in the EOY fluorescence activity, the EOY data provide an unequivocal demonstration of the forward fluorescence interference in UV—vis measurements of fluorescent samples.

The spectral distortion introduced by the scattering and fluorescence interference is shown by comparing the UV-vis spectra obtained from KMnO<sub>4</sub>, EOY, and fPSNP<sub>180</sub>, each with two different concentrations (Figure S2). The experimental UV-vis of KMnO<sub>4</sub> with different concentrations differ only in their spectral intensity, provided the extinction spectrum is within the instrument LDR. In contrast, the UV-vis spectra of both EOY and fPSNP exhibit significant spectral distortion that is especially prominent when the measured UV-vis extinction is high. Such spectral distortion can also be seen from the wavelength dependence of the correlation between the experimental UV-vis extinction and the theoretical extinction of EOY and fPSNP<sub>180</sub> samples (Figure 1).

It is not uncommon that researchers attribute the concentration dependent UV-vis spectra of fluorescent

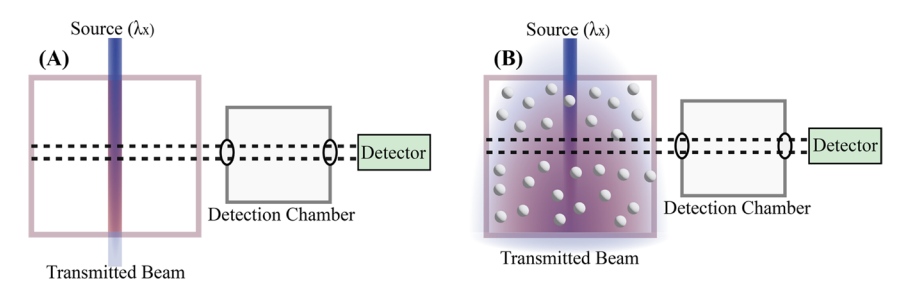


Figure 3. Schematic representation of pinhole effects in (A) scattering-free and (B) scatterer-containing fluorescent samples. The incident and scattered light are in blue, and emitted light is in red. The black dashed region represents the region where fluorescence photons are most effectively collected due to the instrument pinhole effect.

samples to physicochemical interactions among fluorophores or between fluorophores and ligands including nanoscale or larger particles.<sup>25–28</sup> Such a possibility is excluded in this experiment for the samples used in Figure 1. First, the EOY concentration, even in the most concentrated solution, is far below its solubility (1 mg/mL in ethanol). Second, carboxylate fPSNPs used in this work are stable in solutions, and the fluorophores in fPSNP are all impregnated inside a polymer matrix (Figure S3). Therefore, the possibility for strong intermolecular interactions in the EOY sample and interparticle interactions in fPSNP<sub>180</sub> samples should be negligibly small. In other words, the concentration dependence of the EOY and fPSNP UV-vis spectra (Figure 1) must be due predominantly to fluorescence and scattering interference. These observations caution the use of UV-vis spectroscopic analysis of fluorescent samples for both fluorophore quantifications and fluorophore interactions because the upper LDR limit for the fluorescent samples can be significantly smaller than the instrument detection limit that is commonly evaluated using molecular chromophores.

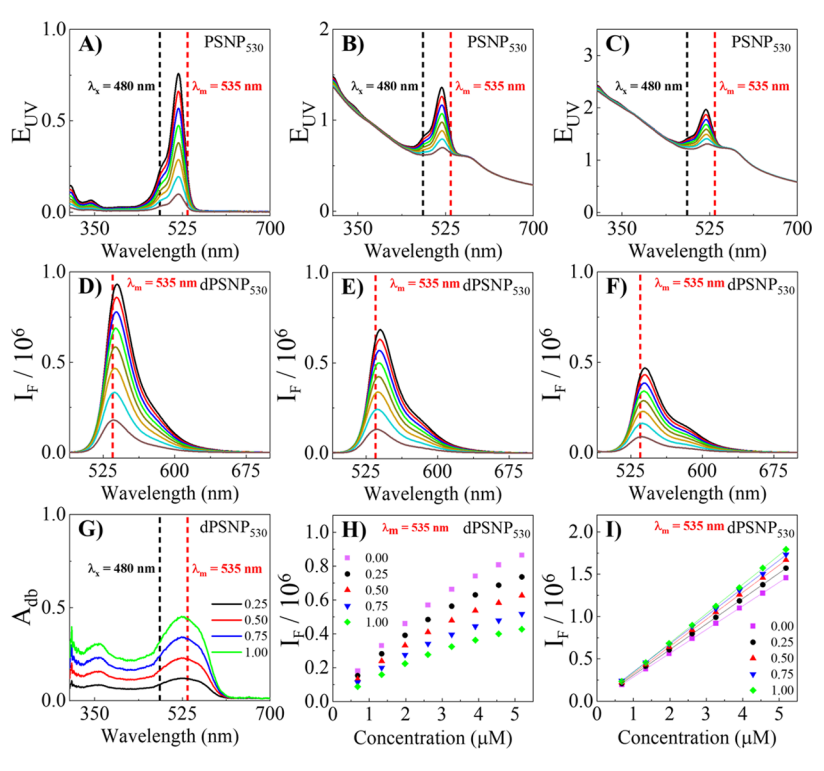
Effect of PSNPs on EOY Fluorescence. Plain PSNPs are approximately pure light scatterers with no significant light absorption or emission in the wavelength region of interest; however, one must ensure that there is no significant physicochemical interactions between EOY and PSNP before using PSNPs to probe the impact of light scattering on EOY fluorescence. Control experiments reveal that EOY has no significant interactions with dialyzed PSNP<sub>100</sub>, PSNP<sub>200</sub>, or PSNP<sub>380</sub>. The UV-vis spectrum of EOY/PSNP solutions prepared with these PSNPs is approximately the same as the sum of the UV-vis spectra acquired with their respective PSNP and EOY controls. In contrast, there is a significant difference between the experimental EOY/PSNP50 UV-vis spectrum and the mathematical sum of the UV-vis spectra of the EOY and dialyzed PSNP<sub>50</sub> controls (Figure S7). It is noted that the maximum UV-vis extinctions for all explored samples (Figure 2, Figures S3-S5) are kept below 2 at 520 nm, the peak EOY absorption wavelength. In this case, the interference of forward scattered or forward fluorescence light to the sample UV-vis measurement should be negligibly small (Figure 1). Therefore, the difference between the experimental UV-vis spectrum of the PSNP<sub>50</sub>/EOY mixture solution and the sum spectrum of the PSNP<sub>50</sub> and EOY controls is a definitive marker of EOY and PSNP<sub>50</sub> interactions with the dialyzed PSNP<sub>50</sub>. To avoid data misinterpretation, the effects of light scattering on fluorophore fluorescence were investigated only with PSNP<sub>100</sub>, PSNP<sub>200</sub>, and PSNP<sub>380</sub> (Figure 2), but not PSNP<sub>50</sub>.

Figure 2 shows three series of example UV-vis extinction spectra (Figure 2A-C) and fluorescence emission spectra (Figures 2D-F) obtained with EOY and EOY/PSNP<sub>380</sub>. Complete sets of UV-vis and fluorescence emission spectra for all EOY/PSNP samples summarized in Figure 2J-L are provided in Figures S4–S6. The as-acquired EOY fluorescence exhibits poor linearity with the EOY concentration (Figure 2G-I) in the EOY controls and all EOY/PSNP solutions. Empirically, however, such nonlinearity can all be corrected by applying the absorption IFE model (eq 2), where  $A_x$  and  $A_m$ used for the absorption IFE correction are the EOY absorbances at the excitation and emission wavelengths, respectively. The  $d_x$  and  $d_m$  are 0.49 and 0.52, respectively; these values were determined using a water Raman method. Indeed, the absorption IFE-corrected fluorescence intensities (Figure 2J-L) all exhibit excellent linearity with the EOY concentration in both EOY and EOY/PSNP solutions.

Cross-examination of the linearly fitting equations in Figure 2J–L is revealing. Evidently, increasing  $PSNP_{100}$  and  $PSNP_{200}$  concentration increases only the intercept of the linearly fitted equation but has no significant effect on the slope of the linear equations. This indicates that the presence of  $PSNP_{100}$  or  $PSNP_{200}$  in the EOY solution has no significant impact on fluorophore emission intensity. However, the intercept of these linear equations increases with an increasing  $PSNP_{100}$  or  $PSNP_{200}$  concentration. This is likely due to PSNP background interference (Figure S8).

Increasing the PSNP<sub>380</sub> concentration increases both the intercepts and slopes of the linear equation obtained for the PSNP<sub>380</sub>/EOY solutions. The enhancement of the intercept is, again, likely due to the PSNP background. However, the increased slopes indicate that PSNP380 scattering enhances the EOY fluorescence emission. Collectively, the data obtained with PSNP<sub>100</sub>, PSNP<sub>200</sub>, and PSNP<sub>380</sub> strongly suggest that only the light scattering by large PSNPs has a significant impact on fluorophore fluorescence. In contrast, the scattering by PSNPs of 200 nm or smaller in diameter has a negligibly small impact on the fluorophore fluorescence emission. This conclusion is also supported by the earlier report that light scattering by 100 nm PSNPs did not have a significant effect on the fluorescence intensity of fluorescent quantum dots, as well as the fPSNPs obtained in this work (vide infra). This fluorescence enhancement by large PSNPs is also consistent with the experimental data obtained with dPSNPs with a nominal diameter of 530 nm (vide infra).

$$I(\lambda_x, \lambda_m) = I(\lambda_x) Q(\lambda_x, \lambda_m) R(\lambda_m) l_s A_{x,f} 10^{-(A_{x,s} d_x + A_{m,s} d_m)}$$
(5)



**Figure 4.** (A–C) UV–vis and (D–F) fluorescence spectra of (A, D) EOY and (B, E), (C, F) EOY/dPSNP<sub>530</sub>. The PSNP<sub>530</sub> concentrations for samples used in (A, D), (B, E), and (C, F) are 0, 1.18, and 2.31 pM, respectively. The EOY concentrations in the sample series are all the same and range from 0.68 to 5.19  $\mu$ M. The excitation wavelength is 480 nm for the fluorescence spectra shown. (G) ISARS-derived double-beam absorbance for dPSNP<sub>530</sub> used for the EOY/dPSNP<sub>530</sub> solutions. (H, I) As-acquired and absorption IFE-corrected fluorescence intensity as a function of EOY concentration. Complete data for all EOY/dPSNP<sub>530</sub> solutions are shown in Figure S9.

Mechanistically, the effect of light scattering on fluorophore fluorescence can be explained by visiting a first-principles model we developed recently for correlating fluorophore fluorescence  $I(\lambda_x, \lambda_m)$  acquired with a conventional spectrofluorometer (eq 5) for scattering-free fluorescence samples.  $I(\lambda_x)$  represents the excitation intensity, and  $A_{x,s}$  and  $A_{m,s}$  are sample light absorbances at the excitation and emission wavelengths, respectively. For samples that contain only the molecular fluorophores,  $A_{x,s}$  and  $A_{m,s}$  are equivalent to  $A_{x,f}$  and  $A_{m,p}$  respectively.  $A_{x,p}$  stands for the fluorophore absorbance at the excitation wavelength.  $Q(\lambda_x, \lambda_m)$  represents the quantum yield of the fluorophore at the specified excitation and emission wavelength.  $R(\lambda_m)$  summarizes the instrument responsivity in the detection of emitted photons.  $l_s$  is the effective sampling path length. Due to the instrument pinhole effect, shown schematically in Figure 3, only the fluorescence signal generated within this effective sampling path length contributes significantly to the experimental fluorescence spectrum. The effective sampling volume for scatterer-free solutions must be smaller than that for scatterer-containing samples due to the scattering diversity of the optical path from the otherwise collimated beam (Figure 3). This enhancement of the effective sampling volume can also be viewed as the enhancement of the absorption path length for excitation photons entering the effective sampling path length  $l_s$ . For the scatterer-free sample, the effective absorption path length is equal to the effective sampling path length l<sub>s</sub>. However, for scatterer-containing samples, the effective absorption path length is  $k_S l_s$  where  $k_S \ge 1$ .

The net effect of light scattering on fluorescence depends on two competing factors: the absorption path length inside the sampling volume that increases the possibility of the excitation to generate fluorescence emission, and the scattering IFE that reduces the number of photons entering the sampling volume. Such scattering IFE has been shown in Part I of this series of companion articles and is manifested by both scattering extinction and intensity measurements.<sup>1</sup>

It is emphasized that scattering IFE is extraordinarily complex, and it depends on not only the sample scattering extinction but also its scattering depolarization. Compared with the absorption IFE, however, scattering IFE is drastically smaller. Herein we use  $\eta_S$  to present the scattering IFE scattering on the fluorophore fluorescence.

Equation 6 represents the revised model for scatterercontaining fluorescent samples. The only difference between eq 6 and eq 5 is the  $k_S$  and  $\eta_S$  terms discussed in the preceding sections.

$$I(\lambda_x, \lambda_m) = I(\lambda_x) Q(\lambda_x, \lambda_m) R(\lambda_m) k_S l_s A_{x,f} 10^{-(A_{x,s}d_x + A_{m,s}d_m) - \eta_S}$$
(6)

Under the condition where scattering IFE is small ( $\eta_S$  < 0.05), eq 6 can be simplified into eq 7 where  $\beta_S$  is the scatterer-dependent constant. This constant can also be viewed as a scattering-dependent correction factor for light absorption inside the effective sampling volume.

$$I(\lambda_x, \lambda_m) = I(\lambda_x) Q(\lambda_x, \lambda_m) R(\lambda_m) \beta_S l_s A_{x,f} 10^{-(A_{x,s}d_x + A_{m,s}d_m)}$$
(7)

Combining eq 2 and eq 7 leads to eq 8, showing that the absorption IFE-corrected fluorescence intensity is linearly correlated with the fluorophore absorbance  $A_{x,p}$  as well as to eq 9 by replacing  $A_{x,f}$  with the fluorophore concentration using Beer's law and using  $K(\lambda_m)$  as  $R(\lambda_m)\varepsilon_f b$ 

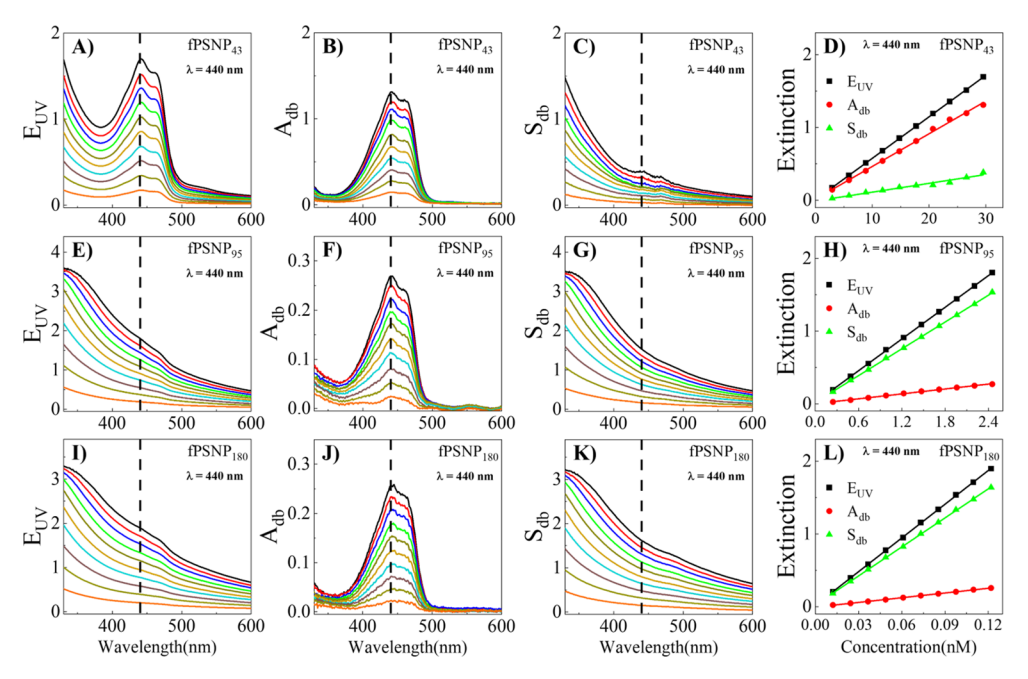


Figure 5. (A, E, I) Experimental extinction spectra of fPSNP<sub>43</sub>, fPSNP<sub>95</sub>, and fPSNP<sub>180</sub>, respectively. (B, F, J) UV-vis absorption extinction spectra derived from ISARS-based absorbance spectra for the samples shown in (A), (E), and (I), respectively. (C, G, K) UV-vis scattering extinction spectra of fPSNP<sub>43</sub>, fPSNP<sub>95</sub>, and fPSNP<sub>180</sub> samples, which were obtained by subtracting the experimental extinction spectra in (A), (E), and (I) by the corresponding absorption extinction spectra in (B), (F), and (J), respectively. (D, H, L) UV-vis total extinction, absorption extinction, and scattering extinction intensity at 440 nm for the fPSNP<sub>43</sub>, fPSNP<sub>95</sub>, and fPSNP<sub>180</sub>, respectively.

$$I^{corr}(\lambda_x, \lambda_m) = I(\lambda_x)Q(\lambda_x, \lambda_m)R(\lambda_m)\beta_S l_s C_f$$
(8)

$$I^{corr}(\lambda_x, \lambda_m) = I(\lambda_x)Q(\lambda_x, \lambda_m)K(\lambda_m)\beta_S l_s C_f$$
(9)

The near perfect linearity of the experimental data obtained with EOY/PSNP provides empirical validation of eq 9 for correlating the sample fluorescence intensity with fluorophore concentration. Therefore, eq 9 is a generalized model for correlating the sample fluorescence and fluorophore concentration in solutions containing both absorption and scatterers.  $\beta_{\rm S}$  is approximately 1 for EOY mixed with both PSNP<sub>100</sub> (Figure 2J) and PSNP<sub>200</sub> (Figure 2K), indicating that the two competing factors by light scattering on EOY fluorescence cancel each other. This conclusion is consistent with our earlier report that the scattering by PSNP<sub>100</sub> has no significant impact on quantum dots fluorescence. However, the  $\beta_S$  value is invariably larger than 1 for EOY/PSNP<sub>380</sub>, and it increases with increasing PSNP<sub>380</sub> scattering extinction (Figure 2L). This observation indicates the absorption path length enhancement by PSNP<sub>380</sub> is more significant than its scattering IFE. This result is consistent with the fact that the scattering IFE is much more significant for PSNP<sub>100</sub> and PSNP<sub>200</sub> than for PSNP<sub>380</sub>. The fact that light absorption and scattering can both change fluorophore fluorescence in totally different ways (attenuate or enhance) demonstrates the complexity of fluorescence spectroscopic analysis of turbid samples.

Effect of dPSNP on EOY Fluorescence. The dPSNP<sub>530</sub> used in this work are simultaneous light absorbers and scatterers with no significant fluorescence activities.<sup>2</sup> The asacquired EOY fluorescence decreases with increasing dPSNP<sub>530</sub> concentration (Figure 4A–F, H). After the absorption IFE on EOY fluorescence is corrected, however, EOY fluorescence increases with increasing dPSNP<sub>530</sub> concentration (Figure 4I). This observation indicates that, while the dPSNP<sub>530</sub> light absorption reduces EOY fluores-

cence, its scattering enhances the fluorescence intensity. It is noted that the  $A_{x,s}$  and  $A_{m,s}$  values used for absorption IFE correction are the sum of the EOY and dPSNP absorbances at the excitation and the emission wavelengths, respectively. Therefore, one must obtain the dPSNP absorbance spectra (Figure 4G) before the absorption IFE correction. The experimental separation of the dPSNP extinction spectrum into its absorption and extinction component spectra was recently reported in Part II.<sup>2</sup>

The data obtained with the dPSNP allow us to make a headto-head comparison of the impact of light absorption and scattering on fluorophore fluorescence. dPSNP<sub>530</sub> is primarily a light scatterer at the excitation wavelength (480 nm; Figure 4). Its absorption extinction-to-scattering extinction ratio at 480 nm is 0.3436. However, the overall effects of dPSNP on the asacquired EOY fluorescence are dominated by its light absorption. The impact of light scattering by dPSNP<sub>530</sub> is evident only in the absorption IFE-corrected spectra. This highlights the importance of separating sample absorption and scattering in the discussion of the sample UV-vis extinction of fluorescence measurements. Unfortunately, in the current literature, the impacts of sample light scattering and absorption on fluorescence measurements have either not been considered at all or their impacts have been assumed to be the same by using UV-vis extinction for sample IFE correction. 29-33

**Optical Properties of fPSNPs.** fPSNPs are made with molecular fluorophores dispersed in a polystyrene matrix. They are simultaneous light absorbers, scatterers, and emitters at the wavelength at which fPSNP absorbs. While the PSNP matrix is approximately pure scatterers, quantification of the absorption and fluorescence activities of the impregnated fluorophores, to our knowledge, is not available.

The experimental separation of light scattering and absorption contributions to the fPSNP UV—vis extinction spectra (Figure 5) is performed using the recent ISARS

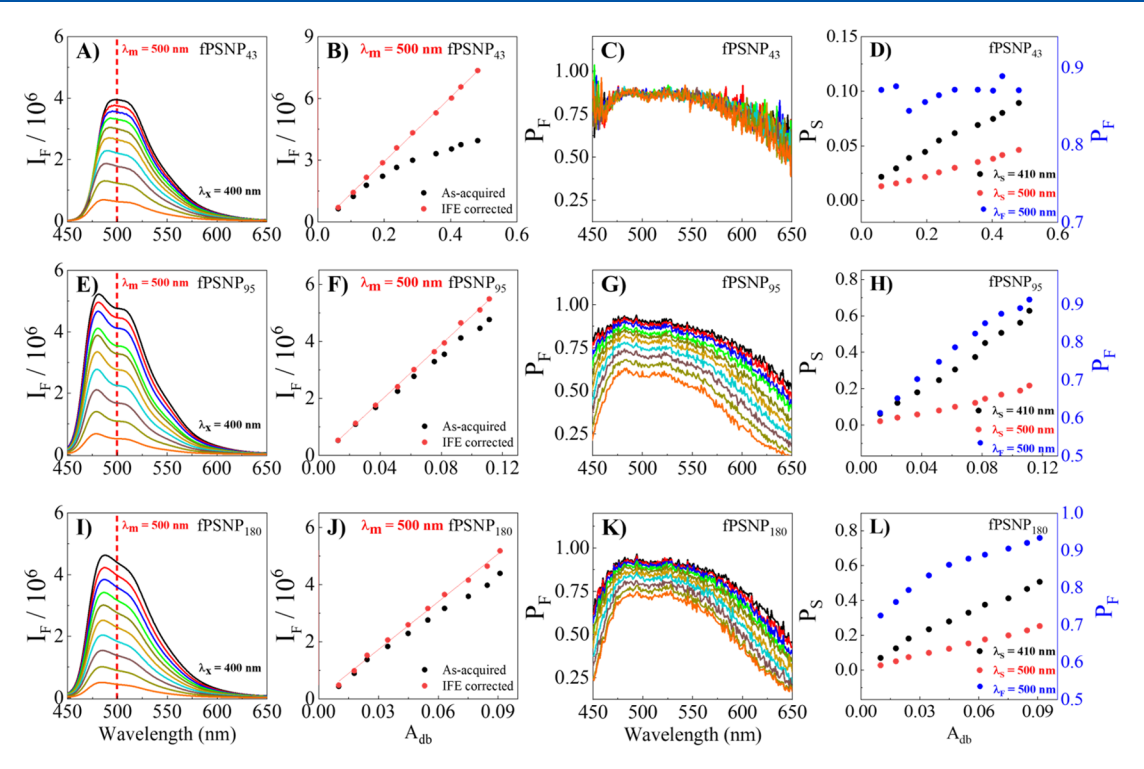


Figure 6. (A, E, I) Fluorescence emission spectra of fPSNP<sub>43</sub>, fPSNP<sub>95</sub>, and fPSNP<sub>180</sub>, respectively. (B, F, J) (Black dots) As-acquired and (Red dots) absorption IFE-corrected fluorescence intensity as a function of fPSNP<sub>43</sub>, fPSNP<sub>95</sub>, and fPSNP<sub>180</sub> absorption extinction at the excitation wavelength, respectively. (C, G, K) Fluorescence emission depolarization spectra of the fPSNP<sub>43</sub>, fPSNP<sub>95</sub>, and fPSNP<sub>180</sub> samples, respectively. (D, H, L) Scattering depolarization at 400 and 500 nm and fluorescence depolarization at 500 nm as a function of the fPSNP scattering extinction at the excitation wavelength. The as-acquired linearly polarized spectra for light scattering and fluorescence depolarization quantification are shown in Figures S12 and S13.

method.<sup>2,34</sup> The complete data sets for the as-acquired ISARS intensity spectra, ISARS-based absorbance, and ISARS-derived double-beam absorbance spectra are shown in Figures S10 and S11. The effectiveness of ISARS for the quantification of sample absorption and scattering extinction is shown by the near perfect linear dependence of experimental total extinction, absorption extinction, and scattering extinction on the fPSNP concentration (Figure 5D, H, L). It is noted that to avoid the interference of forward scattered light in the UV—vis spectral measurement, the UV—vis extinction intensities of all fPSNP solutions were kept below 2 at the excitation wavelength.

The UV-vis extinction spectra of the fPSNPs (Figure 5A, E, I) are different, which is not surprising due to the strong size dependence of light scattering. However, the absorbance spectra (Figure 5B, F, J) of the fPSNPs of three different sizes bear high similarity, which is consistent with the fact that the fluorophores inside these fPSNPs are the same according to the vendor. By assuming that the absorption activities of the fluorophores imbedded inside fPSNPs are the same, we estimate both the relative fluorophore-to-fPSNP number ratio and the fluorophore volume density in the polystyrene matrix for fPSNPs of different sizes. The relative fluorophore-tofPSNP number ratios are 1, 2.4, and 42.6 for fPSNP<sub>43</sub>, fPSNP<sub>95</sub>, and fPSNP<sub>180</sub>, respectively, while their relative fluorophore volume densities are 1, 0.22, and 0.58. In other words, the fluorophores are most densely packed inside fPSNP<sub>43</sub>.

In contrast to the high similarity of the UV—vis absorption extinction spectra among fPSNP<sub>43</sub>, fPSNP<sub>95</sub>, and PSNP<sub>180</sub>, the shapes of the emission spectra for these fPSNPs are somewhat different, specifically between the fPSNP<sub>43</sub> spectrum and those

of fPSNP<sub>95</sub> and PSNP<sub>180</sub>. Further, the fluorescence activity of the fluorophore inside fPSNP43 is also significantly different from those inside fPSNP<sub>95</sub> and fPSNP<sub>180</sub> (Figure 6A, B, E, F, I, J). The quantum yield of the fluorophore inside the PSNP matrix is proportional to the slope of the linear curve between the absorption IFE-corrected fluorescence intensity and the fluorophore absorbance at the excitation wavelength (eq 8). The relative fluorescence activities of the fPSNP<sub>95</sub> and fPSNP<sub>180</sub> are very similar, and they are ~1.8 times higher than that of fPSNP43. This conclusion is consistent with the fluorescence lifetimes quantified for these fPSNPs (Figure S14). The average lifetimes of fPSNP<sub>43</sub>, fPSNP<sub>95</sub>, and  $\text{fPSNP}_{180}$  are 62.96  $\pm$  0.36, 48.22  $\pm$  0.64, and 48.49  $\pm$  0.42 ns. Assuming that the nonradiative decay rate constant is the same for the fluorophore impregnated inside the fPSNPs of different sizes, the fluorescence quantum yields then increase with increasing radiative decay rate constant or decreasing lifetimes. One likely reason for the quantum yield differences among these fPSNPs is that the fluorophore packing density inside fPSNP<sub>43</sub> is too high. When the intermolecular distance is shorter than a certain threshold volume, the fluorophore fluorescence activities decrease because dipole-dipole interactions among the neighboring fluorophores enhance nonradiative decays of the excited fluorophores. 35-38

Cascading light scattering can enhance both scattering and fluorescence depolarizations. Such an effect is especially evident for fPSNP<sub>95</sub> and fPSNP<sub>180</sub>. The fPSNP<sub>43</sub>, fPSNP<sub>95</sub>, and fPSNP<sub>180</sub> scattering depolarization spectra are quantified using the linearly polarized resonance spectroscopic method, while the fPSNP<sub>43</sub>, fPSNP<sub>95</sub>, and fPSNP<sub>180</sub> fluorescence depolarization spectra (Figure 6C, J, K, respectively) are

acquired using linearly polarized fluorescence measurements. 12,39 Mechanistically, the fluorescence depolarization increases with the fPSNP concentration due to multiple combined effects. First, depolarization increases with increasing scatterers' concentration. Any fluorescence generated by absorbing scattered light and the scattering of emitted photons enhances fluorescence depolarizations. Second, any cascading fluorophore absorption, emission, reabsorption, and reemission processes will increase the fluorescence depolarization. The depolarization of the re-emitted photons must be higher than that of the initial emitted photons.

#### CONCLUSIONS

The current work focuses on cascading optical processes and their impacts on the spectroscopic characterization of fluorescence samples. A generalized model is developed for a mechanistic understanding of how forward scattered and emitted light interferes with UV-vis measurements to deviate from Beer's law, causing spectral distortions of fluorescence and/or scattering samples. The interplay among absorption, scattering, and fluorescence emission is explored through three sets of samples including a fluorophore and PSNP mixture, a mixture of a fluorophore with dyed PSNPs, and fluorescence nanoparticles that act as simultaneous absorbers, scatterers, and emitters. The absorption IFE-corrected fluorophore fluorescences all exhibited excellent linearity with the fluorophore absorbance (or equivalently, to the fluorophore concentration). While the light absorption by the nonfluorogenic dye invariably reduces the sample fluorescence by exerting the absorption IFE, the impact of light scattering on the fluorophore fluorescence depends on two competing factors: the scattering IFE that reduces the fluorescence intensity and the absorption path length enhancement inside the effective sampling volume, which can enhance fluorescence emission. The combined ISARS, LRPS, and fluorescence measurements enabled experimental quantification of the UVvis absorption, scattering, and fluorescence activities of fluorescence nanoparticles. These spectroscopic data also allowed quantification of the scattering and fluorescence depolarizations as a function of the concentration of the fluorescent nanoparticles. Although it is expected that the findings of this study will be applicable to all relatively low optical light fluorescent samples with an optical density of 2 or less, further studies will be needed to determine their relevance for optically dense samples.

## ASSOCIATED CONTENT

## **Supporting Information**

The Supporting Information is available free of charge at https://pubs.acs.org/doi/10.1021/acs.analchem.3c00823.

Derivation of eq 3; completed UV—vis and emission spectra of EOY/PSNP and EOY/dPSNP solutions; PSNP fluorescence background spectrum; and ISARS and fluorescence lifetime analyses of fPSNPs (PDF)

#### AUTHOR INFORMATION

## **Corresponding Author**

Dongmao Zhang — Department of Chemistry, Mississippi State University, Mississippi State, Mississippi 39762, United States; orcid.org/0000-0002-2303-7338; Phone: (662)-325-6752; Email: dongmao@chemistry.msstate.edu

#### **Authors**

Max Wamsley — Department of Chemistry, Mississippi State University, Mississippi State, Mississippi 39762, United States; © orcid.org/0000-0001-6790-4846

Pathum Wathudura — Department of Chemistry, Mississippi State University, Mississippi State, Mississippi 39762, United States; oocid.org/0000-0003-3846-812X

Samadhi Nawalage — Department of Chemistry, Mississippi State University, Mississippi State, Mississippi 39762, United States

Shengli Zou — Department of Chemistry, University of Central Florida, Orlando, Florida 32816, United States;
orcid.org/0000-0003-1302-133X

Complete contact information is available at: https://pubs.acs.org/10.1021/acs.analchem.3c00823

#### **Author Contributions**

\*M.W., P.W., and S.N. contributed equally.

#### Notes

The authors declare no competing financial interest.

#### ACKNOWLEDGMENTS

This work was supported in part by the Center of Biomedical Research Excellence Program funded through the Center for Research Capacity Building in the National Institute for General Medical Sciences (P20GM103646) and by an NSF Grant (CHE 2203571). S.Z. is grateful for the support from NSF (DMR- 2004546) and the Extreme Science and Engineering Discovery Environment (XSEDE) as the service provider through allocation to S.Z. The content is solely the responsibility of the authors and does not necessarily represent the official views of the National Institutes of Health or National Science Foundation.

#### REFERENCES

- (1) Nawalage, S.; Wathudura, P.; Wang, A.; Wamsley, M.; Zou, S.; Zhang, D. Anal. Chem. 2023, 95 (3), 1899–1907.
- (2) Wathudura, P.; Wamsley, M.; Wang, A.; Chen, K.; Nawalage, S.; Wang, H.; Zou, S.; Zhang, D. *Anal. Chem.* **2023**, *95* (9), 4461–4469.
- (3) Soos, M.; Lattuada, M.; Sefcik, J. J. Phys. Chem. B 2009, 113 (45), 14962-14970.
- (4) Oelkrug, D.; Brun, M.; Rebner, K.; Boldrini, B.; Kessler, R. Appl. Spectrosc. 2012, 66 (8), 934–43.
- (5) Lakowicz, J. R. Principles of fluorescence spectroscopy; Springer: 2006.
- (6) Valeur, B.; Berberan-Santos, M. N. Molecular Fluorescence: Principles and Applications, 2nd ed.; Wiley-VCH Verlag GmbH & Co. KGaA: 2012.
- (7) Wamsley, M.; Nawalage, S.; Hu, J.; Collier, W. E.; Zhang, D. Anal. Chem. **2022**, 94 (19), 7123–7131.
- (8) Nettles, C. B., II; Hu, J.; Zhang, D. Anal. Chem. 2015, 87 (9), 4917–4924.
- (9) Xu, J. X.; Vithanage, B. C. N.; Athukorale, S. A.; Zhang, D. Analyst. 2018, 143 (14), 3382–3389.
- (10) Leese, R. A.; Wehry, E. L. Anal. Chem. 1978, 50 (8), 1193-
- (11) Siano, S. A. J. Quant. Spectrosc. Radiat. Transfer 1992, 47 (1), 55-73.
- (12) Xu, J. X.; Siriwardana, K.; Zhou, Y.; Zou, S.; Zhang, D. Anal. Chem. **2018**, 90 (1), 785–793.
- (13) Xu, J. X.; Hu, J.; Zhang, D. Anal. Chem. 2018, 90 (12), 7406-7414.
- (14) Kong, J.; Zhang, J.; Wang, Y.; Qi, W.; Rao, H.; Hu, L.; Su, R.; He, Z. ACS Appl. Mater. Interfaces. 2020, 12 (4), 4212–4220.

- (15) Han, Y.; Lv, W.; Chen, H.; Li, H.; Chen, J.; Li, Z.; Qiu, H. Anal. Chem. 2020, 92 (5), 3949–3957.
- (16) Saladino, G. M.; Vogt, C.; Li, Y.; Shaker, K.; Brodin, B.; Svenda, M.; Hertz, H. M.; Toprak, M. S. ACS Nano 2021, 15 (3), 5077-5085.
- (17) Ong, S. Y.; Zhang, C.; Dong, X.; Yao, S. Q. Angew. Chem. 2021, 60 (33), 17797–17809.
- (18) Li, W.; Kaminski Schierle, G. S.; Lei, B.; Liu, Y.; Kaminski, C. F. Chem. Rev. **2022**, 122 (15), 12495–12543.
- (19) Pahari, S. K.; Olszakier, S.; Kahn, I.; Amirav, L. Chem. Mater. **2018**, 30 (3), 775–780.
- (20) Zhu, Z.; Tian, D.; Gao, P.; Wang, K.; Li, Y.; Shu, X.; Zhu, J.; Zhao, Q. JACS. 2018, 140 (50), 17484–17491.
- (21) Caponetti, V.; Trzcinski, J. W.; Cantelli, A.; Tavano, R.; Papini, E.; Mancin, F.; Montalti, M. Front. Chem. 2019, 7, No. 168.
- (22) Fang, Y.; Xing, C.; Zhan, S.; Zhao, M.; Li, M.; Liu, H.; Wang, C. ACS Biomater. Sci. Eng. **2019**, 5 (12), 6779–6793.
- (23) Zhang, J.; Fang, F.; Liu, B.; Tan, J.-H.; Chen, W.-C.; Zhu, Z.; Yuan, Y.; Wan, Y.; Cui, X.; Li, S.; Tong, Q.-X.; Zhao, J.; Meng, X.-M.; Lee, C.-S. ACS Appl. Mater. Interfaces. 2019, 11 (44), 41051–41061.
- (24) Zhao, Y.; Hu, Y.; Zhong, Y.; Wang, J.; Liu, Z.; Bai, F.; Zhang, D. J. Phys. Chem. C **2021**, 125 (40), 22318–22327.
- (25) Nagai, A.; Miyake, J.; Kokado, K.; Nagata, Y.; Chujo, Y. *JACS*. **2008**, *130* (46), *15276*–*15278*.
- (26) Choi, Y.-J.; Luo, T.-J. M. ACS Appl. Mater. Interfaces. 2009, 1 (12), 2778–2784.
- (27) Santos, P. J.; Macfarlane, R. J. JACS. 2020, 142 (3), 1170-1174.
- (28) Wang, J.; Zhang, C.; Liu, Z.; Li, S.; Ma, P.; Gao, F. Anal. Chem. **2021**, 93 (41), 13755–13764.
- (29) Pan, D.; Liang, P.; Zhong, X.; Wang, D.; Cao, H.; Wang, W.; He, W.; Yang, Z.; Dong, X. ACS Appl. Bio. Mater. **2019**, 2 (3), 999–1005.
- (30) Kharey, P.; Dutta, S. B.; M, M.; Palani, I. A.; Majumder, S. K.; Gupta, S. *Nanotechnology.* **2020**, *31* (9), No. 095705.
- (31) Zhang, W.; Li, Y.; Xu, L.; Wang, D.; Long, J.; Zhang, M.; Wang, Y.; Lai, Y.; Liang, X.-J. ACS Appl. Poly. Mater. **2020**, 2 (10), 4180–4187.
- (32) Siddiquee, S.; Saallah, S.; Bohari, N. A.; Ringgit, G.; Roslan, J.; Naher, L.; Hasan Nudin, N. F. *Nanomaterials.* **2021**, *11* (5), 1142.
- (33) Zhu, Y.; Wang, Z.; Zhao, R.; Zhou, Y.; Feng, L.; Gai, S.; Yang, P. ACS Nano 2022, 16 (2), 3105-3118.
- (34) Wamsley, M.; Wathudura, P.; Hu, J.; Zhang, D. Anal. Chem. **2022**, 94 (33), 11610–11618.
- (35) Gaudreau, L.; Tielrooij, K. J.; Prawiroatmodjo, G. E. D. K.; Osmond, J.; de Abajo, F. J. G.; Koppens, F. H. L. *Nano Lett.* **2013**, *13* (5), 2030–2035.
- (36) Hu, Q.; Jin, D.; Xiao, J.; Nam, S. H.; Liu, X.; Liu, Y.; Zhang, X.; Fang, N. X. Proc. Natl. Acad. Sci. U. S. A. 2017, 114 (38), 10017–10022.
- (37) Singh, P.; Joshi, J. J. Lumin. 2018, 203, 331-335.
- (38) Singh, M. R.; Guo, J.; Fanizza, E.; Dubey, M. J. Phys. Chem. C 2019, 123 (15), 10013-10020.
- (39) Xu, J. X.; Liu, M.; Athukorale, S.; Zou, S.; Zhang, D. ACS Omega. 2019, 4 (3), 4739–4747.